JOC The Journal of Organic Chemistry

pubs.acs.org/joc Note

Alkyl-Substituted Cucurbit[6]uril Bridged β-Cyclodextrin Dimer Mediated Intramolecular FRET Behavior

Fang-Fang Shen, Ying-Ming Zhang, Xian-Yin Dai, Hao-Yang Zhang, and Yu Liu*

Cite This: J. Org. Chem. 2020, 85, 6131−6136 Read Online

ACCESS | Metrics & More | Article Recommendations | Supporting Information

ABSTRACT: A novel triazolyl bridged cucurbituril (CB)−cyclodextrin (CD) dimer was synthesized via click reaction of monopropargyl modified octamethylcucurbit[6]uril and mono-6-azido-β-cyclodextrin. Moreover, it could form stable supramolecular inclusion complexes possessing efficient fluorescence resonance energy transfer, which benefited from the fact that CD and CB can bind amantadine- and pyridinium-containing fluorophores simultaneously. The supramolecular inclusion complex behaviors were investigated by NMR spectroscopy, UV−vis absorption, and fluorescence spectroscopy.

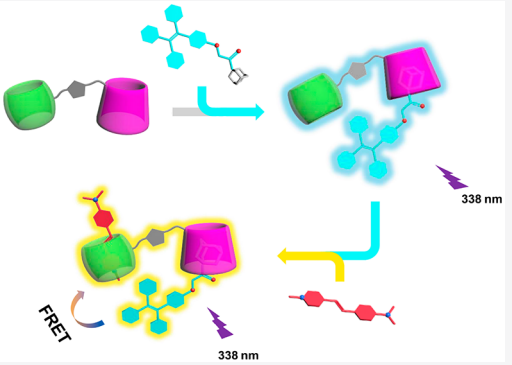

Cucurbit[n]urils (CB[n]s, n = 5−8, 10, 14) are a class of synthetic macrocyclic host molecules consisting of n glycoluril units with a hydrophobic cavity and two identical carbonyl-fringed portals.[1] Although (CB[n]s) are potentially used as a type of host receptor,[2] their practical applications in chemistry, biology, and material areas have been limited, probably due to the insufficient solubility and the difficulty of introducing functional groups on their surfaces. Since the discovery of the first fully alkyl-substituted CB[5], decamethylcucurbit[5]uril, in 1992,[3] a series of fully and partially alkyl-substituted cucurbit[n]uril (SCB[n]) derivatives have been reported successively.[4−6] The physical and chemical properties of alkyl-substituted CB[n]s have been changed, such as cavity size, shape, and electron cloud density of carbonyl oxygen atoms, which increased the solubility in common solvents and produced other special functional properties. The introduction of functional groups on skeletons of CB[n]s has been a huge challenge in CB[n] chemistry due to the chemical stability of CB[n]s. In 2003, Kim and co-workers first prepared a series of CB[n] derivatives, hydroxy-substituted $(HO)_{2n}$CB-[n]s, by simple oxidation of the native CB[n]s with $K_2S_2O_8$ in water,[7] and this served as an accelerator for the application of functionalized CB[n]s in vesicles, polymers, nanomaterials, artificial ion channels, and so on.[8−13] However, the yields for alkyl-substituted CB[n]s in this method was too low for practical use. In 2016, Bardelang and Ouari reported a photochemical method by UV and hydrogen peroxide to introduce a limited number of alcohol functional groups on CB[n]s (n = 5, 6, 7, and 8).[14] Although they have made a correction of conversions from 95% to 100% to 20−40%,[15] this method can be applied to other selected CB[n]s, including alkyl-substituted CB[n]s. However, the functionalization of alkyl-substituted CB[n]s is still rarely reported.[16,17]

On the other hand, due to the importance of photophysical properties, fluorescence resonance energy transfer (FRET) is a research hotspot for scientists in miscellaneous fields. The occurrence of a more effective FRET phenomenon requires some criteria. That is, a FRET system includes at least two chromophores, the donor and the acceptor, which should be located in close proximity and the fluorescence emission spectrum of donor should sufficiently fall into the absorption spectrum of acceptor. However, there are still several defects in the constructing FRET materials, such as the lack of controllability of the covalently connected donor and acceptor, the insufficient solubility in aqueous solution, and the weak interaction between independent fluorophores. Remarkably, through flexible and controllable regulation of the interaction between donor and acceptor pairs, the FRET systems constructed in the form of supramolecular host−guest chemistry could serve as a promising tool to solve these drawbacks. As a result, many interesting supramolecular FRET systems have been constructed and applied in various fields.[18] For instance, Zhou and Yang exhibited a acid/base-controllable FRET system by a host−guest complex between a rhodamine B functionalized pillar[5]arene and cyano-modified

Received: December 30, 2019
Published: April 8, 2020

https://dx.doi.org/10.1021/acs.joc.9b03513
J. Org. Chem. 2020, 85, 6131−6136

Scheme 1. Schematic Illustration of the Structural Formulas of H, G1, and G2 Molecules

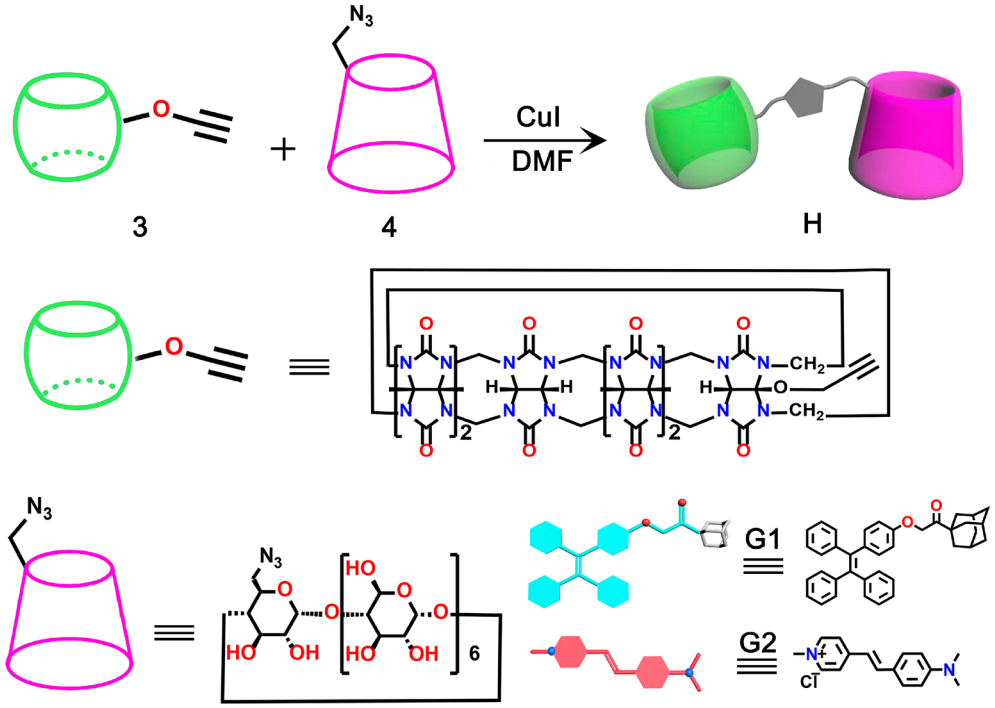

boron dipyrromethene.[19] Park and Kim reported a supramolecular nanosystem based on the fusion assay of two different organelles using a novel host–guest pair, cucurbit[7]-uril-Cy3 and adamantane-Cy5 as a FRET pair.[20] Several FRET systems were also constructed in our research group, using the strategy of supramolecular polymers based on host–guest complexation or in a nanosized noncovalent supramolecular assembly.[21,22] However, in a single supramolecular assembled entity, the utilization of two different types of macrocyclic receptors to achieve an efficient FRET process still remains challenging.

In order to study the binding and photophysical behaviors of functionalized SCB[*n*]s, we utilized SCB[*n*]s possessing the OH group at a designated position to yield a special oxidation product, which was inspired by the complementary molecular binding behaviors of CB[*n*]s and cyclodextrins (CDs).[23] In this work, we designed and synthesized a novel macrocyclic dimer **H** (Figures S4–S6, Supporting Information) consisting of a symmetrical octamethylcucurbituril (OMeCB[6]) and *β*-CD, in which two macrocyclic molecules, $(propargyl)_1$OMeCB[6] (Figures S1–S3, Supporting Information) and mono-6-azido-*β*-CD, were convalently conjugated via click reaction. In our case, given that *β*-CD can incorporate neutral guest molecules possessing an adamantyl end with high binding affinity, the adamantyl tetraphenylethylene (**G1**) (Figures S7–S9, Supporting Information) was accordingly synthesized. Meanwhile, OMeCB[6] is capable of encapsulating cationic guests in its hydrophobic cavity and the binding constant between OMeCB[6] and *trans*-4-[4-(dimethylamino)styryl]-1-methylpyridinium chloride (**G2**) can reach up to 10^6 M^{-1} order of magnitude. Further spectroscopic studies have shown that H has the larger binding affinity for these two guest molecules (**G1** and **G2**) than individual macrocycle molecules (CB and CD moieties) (Scheme 1). Due to the superior solubility of macrocyclic dimers in **H**, an intramolecular FRET system mediated by the conjugation of CB with CD moieties was achieved in an aqueous solution, and the FRET efficiency was determined to be 70.3%.

To confirm the formation of the host–guest complexes between the OMeCB[6] moiety of **H** and **G2** as well as free OMeCB[6] and **G2**, ^{1}H NMR spectroscopic titrations were first performed by using **G2** as a guest compound and free OMeCB[6] as a model host compound. As shown in Figure S10 (Supporting Information), upon the gradual addition of **G2**, the proton signals of the guest appeared to shift upfield ($\Delta\delta$ = −0.22, −0.83, −0.09, for H_1, H_2, H_3, respectively), suggesting that these protons of the guest were included in the cavity of the OMeCB[6] and were shielded by the OMeCB[6]. In contrast, the signal of H_4, H_5 moved downfield by 0.13 and 0.56 ppm, suggesting that these protons on the guest were excluded at the portals of the OMeCB[6]. Additionally, the NMR assignments were made through ^{1}H–^{1}H COSY experiment (Figure S11, Supporting Information). Moreover, when adding 1.0 equiv of **H** to **G2**, similar ^{1}H NMR complexation induced shifts occurs to protons of **G2** compared with OMeCB[6]/**G2** complex (Figure S12 Supporting Information), indicating that **H** and **G2** could form the same host–guest complex as OMeCB[6]/**G2** complex.

It is known that CB[6] and **G2** guest could form a 1:1 inclusion complex with the absorbance at 450 nm and 270 times fluorescence enhancement at 580 nm.[24] To investigate the binding behavior between the OMeCB[6] moiety of **H** and **G2**, UV–vis absorption and fluorescence experiments were further conducted. As discerned from the UV–vis absorption spectra, a Job plot of OMeCB[6]/**G2** complex showed a 1:1 stoichiometry by plotting the absorbance at 450 nm against the molar fraction of OMeCB[6] and **G2** (Figure S13b, Supporting Information).

For the complexation of **H** and **G2**, the stoichiometry was also determined to be 1:1 based on the fluorescence intensity of **G2** in the presence of **H** (Figure S13a, Supporting

https://dx.doi.org/10.1021/acs.joc.9b03513
J. Org. Chem. 2020, 85, 6131–6136

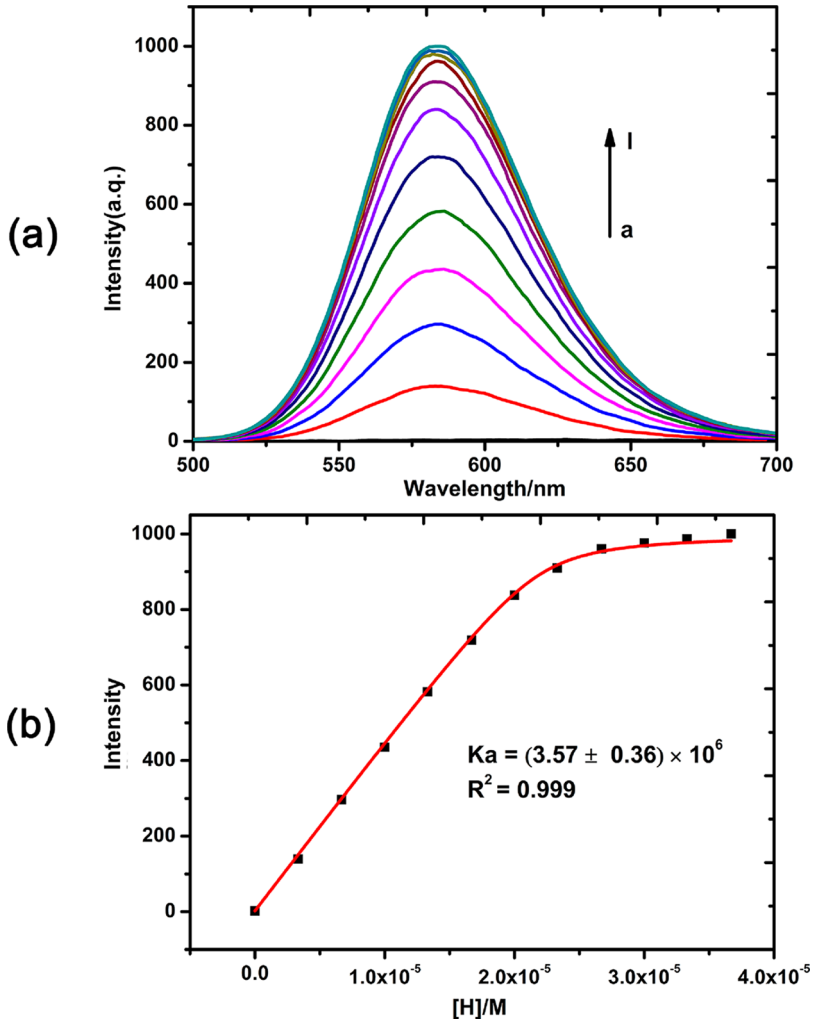

Figure 1. Emission spectra (a) and intensity changes of **G2** at 580 nm (b) upon the gradual addition of **H** in an aqueous solution ([**G2**] = 2×10^{-5} M, [**H**] = $(0–3.67) \times 10^{-5}$ M, 25 °C).

Information). These results also confirmed that the guest molecule **G2** could be exclusively included into the hydrophobic cavity of OMeCB[6] in aqueous solution. Meanwhile, according to the fluorescence spectra, **G2** (20 μM) displayed very poor fluorescence with a maximum emission at 607 nm in aqueous solution, while upon addition of OMeCB[6] or **H** from 0.1 equiv to 1.0 equiv, the emission intensity increased significantly. Additionally, a blue shift from 607 to 582 nm indicated the host–guest interactions between the OMeCB[6] moiety and **G2** (Figures 1a, S14a). The association constant (K_a) of **H**/**G2** was calculated to be 3.57×10^6 M^{-1} by the curve fitting method (Figure 1b). As shown in Figure S14b (Supporting Information), the K_a value for OMeCB[6]/**G2** was 3.22×10^6 M^{-1}, which was consistent with the one in **H**/**G2** complexation.

It is well-known that β-CD could associate with adamantyl guests in aqueous solution. Then, the ^{1}H NMR spectra were utilized by using β-CD and 1-adamanty bromomethyl ketone (**ABK**) as the model compound. The ^{1}H NMR titration spectra for a fixed concentration of **ABK** upon incremental addition of β-CD showed the gradual downfield shifts of adamantyl protons signals (Figure S15, Supporting Information), indicating the inclusion of the adamantyl moiety of the **ABK** guest in the β-CD cavity.[25] Compared with the free β-CD, the ^{1}H NMR spectra also showed that, upon addition of 1.0 equiv of **H**, the peaks of protons $H_{a–c}$ on **ABK** shifted downfield significantly ($\Delta\delta$ = 0.09, 0.08, and 0.22 ppm for $H_{a–c}$, respectively; Figure S16, Supporting Information). Meanwhile, a 2D NOESY NMR spectrum of equimolar **ABK** to **H** that was obtained proved the formation of the host–guest complex. The NOE (nuclear Overhauser enhancement) correlations were observed between adamantyl protons of **ABK** and the β-CD moiety of **H**, corroborating that adamantyl moiety was included in the β-CD's cavity to form the host–guest complex (Figure S17, Supporting Information).

The host–guest complexes of **H**/**G1** and β-CD/**G1** were also studied by UV–vis spectroscopy. From the absorption titration spectra, upon addition of β-CD to an aqueous solution of **G1** with a fixed concentration, the absorbance peak at 345 nm of **G1** experienced a slightly red shift and the absorbance intensity decreased gradually (Figure 2a). The binding constant for the β-CD/**G1** complex was determined to be $(5.38 \pm 0.04) \times 10^3$ M^{-1} (Figure 2b). Compared to the β-CD/**G1** system, the absorption spectra of **H**/**G1** showed quite similar changes. These results revealed that the adamantyl moiety of **G1** was included in the cavity of the β-CD moiety of **H**. In addition, the K_a value of **H**/**G1** was calculated to be $(5.44 \pm 0.16) \times 10^3$ M^{-1}, which was similar to the one of the β-CD/**G2** complex (Figure S18, Supporting Information). In addition, the spectroscopic titration experiments were also

https://dx.doi.org/10.1021/acs.joc.9b03513
J. Org. Chem. 2020, 85, 6131–6136

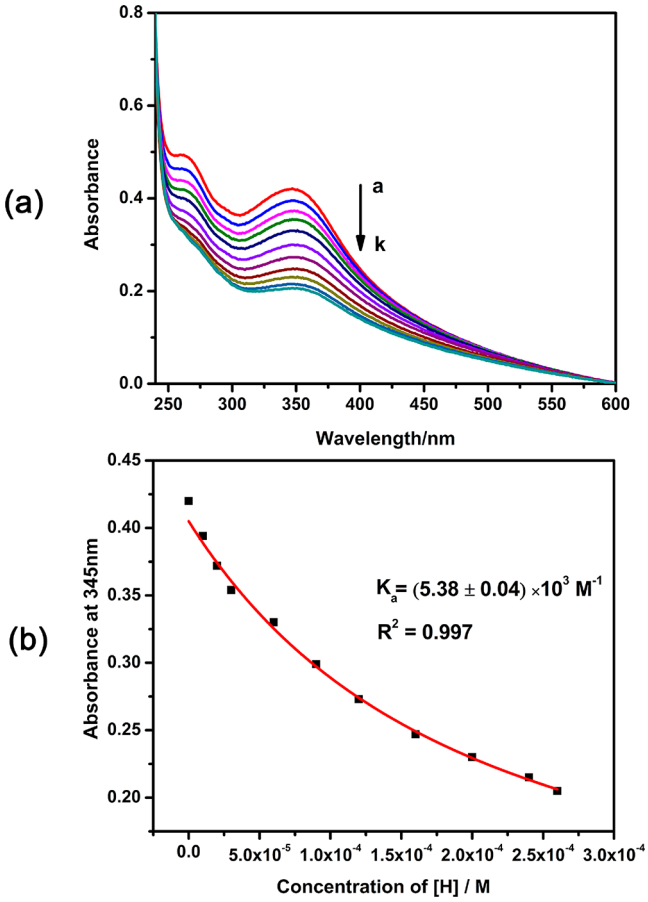

Figure 2. UV−vis spectra (a) and absorbance changes of **G1** at 345 nm (b) upon addition of **H** in an aqueous solution containing 3% DMSO ([**G1**] = 3.0 × 10^{-5} M, [**H**] = (0−2.6) × 10^{-4} M, 25 °C).

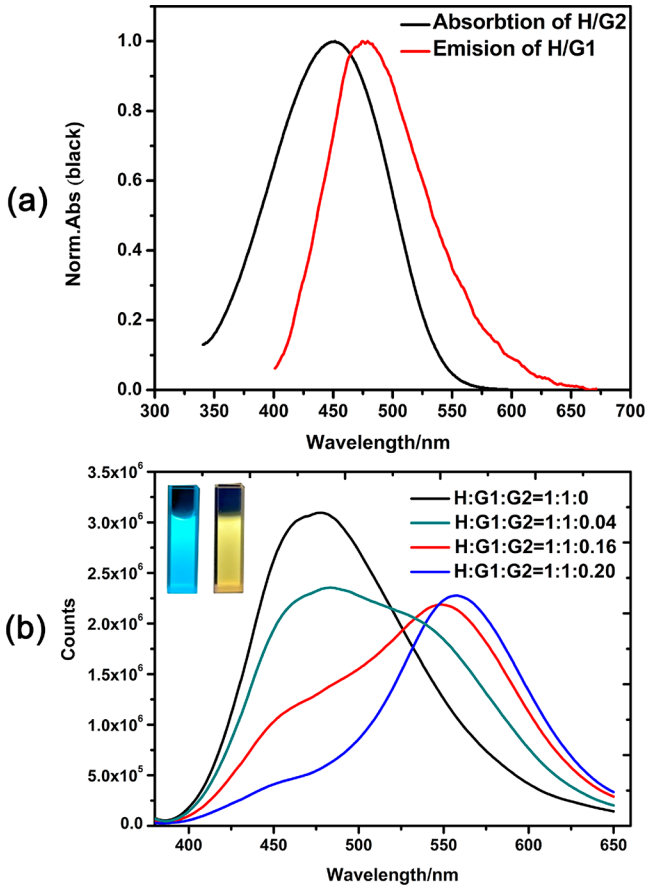

Figure 3. (a) Normalized absorption spectra of **H**/**G2** and emission spectrum of **H**/**G1**. (b) Fluorescence spectra of **H**/**G1** ([**H**] = [**G1**] = 1.0 × 10^{-4} M) in the solution of H_2O/DMSO (97:3) with different concentrations of **G2**. The concentrations of **G2** were 0, 4.0 × 10^{-6}, 1.6 × 10^{-5}, 2.0 × 10^{-5} M, respectively. Inset: left, photographic images of **H**/**G1**; right, **H**/**G1**/**G2** under UV light (365 nm) ([**H**] = [**G1**] = 1.0 × 10^{-4} M, [**G2**] = 2.0 × 10^{-5} M).

performed in D_2O containing 3% DMSO, showing quite similar molecular binding behaviors (Figures S19−S21, Supporting Information).

It is well-known that the fluorescence emission spectrum of donor should sufficiently fall into the UV−vis absorption spectra of the acceptor in an effective FRET process. Theoretical calculation showed that the optimized structure of the inclusion complexes between **H** and two guest molecules (**G1** and **G2**) is appropriate for FRET by the molecular mechanics modeling (Figure S22, Supporting Information). As can be seen in Figure 3a, upon excitation at 338 nm that corresponded to the absorption band of the host−guest complex of **H**/**G1**, the 1:1 supramolecular complex of **H**/**G1** exhibited a strong fluorescence intensity centered around 475 nm in water, which was well overlapped with the absorption band of the **H**/**G2** complex in the range 450−550 nm. To further investigate the FRET process of host−guest complexes based on the macrocyclic dimer, fluorescence titration experiments were conducted in aqueous solution. As shown in Figure 3b, with the stepwise addition of **G2** to the **H**/**G1** (1:1 molar ratio), the fluorescence intensity of **H**/**G1** was gradually decreased along with the enhancement of emission of **H**/**G2** when excited at 338 nm. Meanwhile, the color that corresponded to fluorescence emission was accordingly changed from blue to yellow. In the control experiments, either **H**/**G2** or free **G2** barely gave fluorescence emission in the same experimental conditions (λ_{ex} = 338 nm; Figure S23, Supporting Information). Furthermore, the energy-transfer efficiency was calculated to be as high as 70.3%.

In conclusion, a newly macrocyclic dimer **H** bearing CD and CB moieties was synthesized via click chemistry. OMeCB[6] was chosen to construct this dimer instead of CB[6], because the solubility of parent CB[6] was rather limited in water. Tetraphenylethylene modified with the adamantyl moiety was synthesized to be selectively trapped in the β-CD's cavity. After interaction with the host molecule **H**, there is a strong blue emission centered at 478 nm. Then the **G2** molecule as a receptor could be well encapsulated in the cavity of the OMeCB[6] moiety in an aqueous solution, and the absorption spectrum had a good overlap with the donor emission spectrum. Benefiting the good solubility of this conjugated dimeric host, a newly intramolecular FRET system was constructed conveniently based on the supramolecular host−guest strategy. Therefore, all the research results indicated that novel macrocyclic dimer CB−CD-based host−guest complexation may be significant for designing novel molecular sensors and devices and have potential application in other fields such as materials and biology systems, including drug delivery, cell imaging, and biosensors.

https://dx.doi.org/10.1021/acs.joc.9b03513
J. Org. Chem. 2020, 85, 6131−6136

EXPERIMENTAL SECTION

Preparation of Compound G1. Compound **1**[26] (1.7 g, 4.86 mmol) and 1-adamantyl bromomethyl ketone (1.25 g, 4.86 mmol) were dissolved in acetone (50 mL), and potassium carbonate (2.02 g, 14.58 mmol) was added. The mixture was refluxed using an oil bath overnight. After cooling to room temperature, the solution was filtered, and the filtrate was dried under reduced pressure to remove the solvent. The residue was purified by column chromatography (silica gel, petroleum ether/CH_2Cl_2 = 1:2, v/v) to give compound **1** as a white powder (2.42 g, 95% yield). ^{1}H NMR (400 MHz, DMSO-d_6, TMS): δ1.66 (m, 6H, H of adamantane), 1.82 (m, 6H, H of adamantane), 1.98 (s, 3H, H of adamantane), 4.98 (s, 2H, H of CH_2), 6.60−6.62 (d, J = 8 Hz, 2H, H of benzene), 6.82−6.84 (d, J = 8 Hz, 2H, H of benzene) 6.93−7.18 (m, 14H, H of benzene); ^{13}C {^{1}H} NMR (100 MHz, DMSO-d_6, TMS): δ 27.1, 35.8, 36.9, 44.5, 68.1, 113.7, 126.3, 127.6, 127.8, 130.5, 130.5, 130.6, 131.6, 143.3, 156.3, 208.8 ppm; MS (MALDI) m/z: $[M + H]^+$ Calcd for $C_{38}H_{37}O_2$ 525.30; Found 525.34; $[M + Na]^+$ Calcd for $C_{38}H_{36}O_2Na$ 547.26; Found m/z 547.31. Anal. Calcd for $C_{38}H_{36}O_2$: C, 86.99; H, 6.92; O, 6.10. Found: C, 86.96; H, 6.90; O, 6.09.

Preparation of Compound 3. To a solution of **2**[16] (30 mg, 0.027 mmol) and *N*,*N*′-dihexylviologen bromide salt (13.10 mg, 0.027 mmol), in anhydrous DMSO (2 mL), NaH (10 mg, 0.4 mmol) was added and stirred at room temperature for 15 min. Propargyl bromide (0.5 mL, 5.8 mmol) was added subsequently at 0 °C, and the reaction mixture was stirred at room temperature for 12 h. The reaction was then diluted with 50 mL of diethyl ether and filtered. The remaining solid was triturated with acetone (3 × 50 mL) and dried under vacuum to give a yellow solid (15 mg, 72%). ^{1}H NMR (400 MHz, D_2O): δ 1.78 (m, 24H), 3.01 (s, H), 4.38 (m, 12H), 4.50−4.54 (d, J = 16 Hz, 2H), 5.55 (m, 5H), 5.70 (m, 10H); ^{13}C {^{1}H} NMR (100 MHz, D_2O): δ 15.9, 16.5, 42.9, 44.0, 47.9, 48.1, 52.3, 70.8, 72.5, 77.2, 77.7, 78.0, 97.0, 155.7, 156.8 ppm; HRMS (MALDI) m/z: $[M + Na]^+$ Calcd for $C_{47}H_{54}N_{24}O_{13}Na$ 1185.4200; Found 1185.4198. Anal. Calcd for $C_{47}H_{54}N_{24}O_{13}$: C, 48.54; H, 4.68; N, 28.90. Found: C, 48.52; H, 4.64; N, 28.87.

Preparation of Compound H. CuI (64.48 mg, 0.34 mmol) was added to a solution of **3** (79.02 mg, 0.068 mmol) and **4**[27](78.88 mg, 0.068 mmol) in dry DMF (10 mL), and the reaction mixture was stirred at 80 °C using an oil bath for 24 h under argon. After cooling to room temperature, the mixture was filtered to remove any insoluble copper salt, and the filtrate was evaporated under a reduced pressure to remove excess DMF. The residue was purified by column chromatography (silica gel) with water/acetic acid as eluent to give **H** as a white solid (101 mg, yield 64%). ^{1}H NMR (400 MHz, D_2O): δ 1.68−1.90 (m, 24 H), 3.48−3.96 (m,42 H), 4.25−4.52 (m, 14 H), 4.99−5.10 (m, 7 H), 5.52−5.77 (m, 15 H), 8.16 (s, H); ^{13}C {^{1}H} NMR (100 MHz, D_2O): δ 15.9, 16.5, 42.9, 44.1, 48.2, 51.4, 60.3, 70.4, 70.8, 71.8, 72.0, 72.8, 73.1, 77.8, 78.1, 81.3, 102.0, 156.3 ppm; MS (MALDI) m/z: $[M + Na]^+$ Calcd for $C_{89}H_{123}N_{27}O_{47}Na$ 2344.796; Found 2344.777. Anal. Calcd for $C_{89}H_{123}N_{27}O_{47}$: C, 46.02; H, 5.34; N, 16.28. Found: C, 46.05; H, 5.35; N, 16.30.

ASSOCIATED CONTENT

Supporting Information

The Supporting Information is available free of charge at https://pubs.acs.org/doi/10.1021/acs.joc.9b03513.

Detailed synthesis, characterization data, Job's plots, association constant, absorption and emission spectra, ^{1}H NMR spectra and theoretical calculation (PDF)

AUTHOR INFORMATION

Corresponding Author

Yu Liu − *College of Chemistry, State Key Laboratory of Elemento-Organic Chemistry, Nankai University, Tianjin 300071, China;* orcid.org/0000-0001-8723-1896; Email: yuliu@nankai.edu.cn

Authors

Fang-Fang Shen − *College of Chemistry, State Key Laboratory of Elemento-Organic Chemistry, Nankai University, Tianjin 300071, China*

Ying-Ming Zhang − *College of Chemistry, State Key Laboratory of Elemento-Organic Chemistry, Nankai University, Tianjin 300071, China*

Xian-Yin Dai − *College of Chemistry, State Key Laboratory of Elemento-Organic Chemistry, Nankai University, Tianjin 300071, China*

Hao-Yang Zhang − *College of Chemistry, State Key Laboratory of Elemento-Organic Chemistry, Nankai University, Tianjin 300071, China*

Complete contact information is available at: https://pubs.acs.org/10.1021/acs.joc.9b03513

Notes

The authors declare no competing financial interest.

ACKNOWLEDGMENTS

We thank NNSFC (21432004, 21871154, 21772099, and 21861132001) for financial support.

REFERENCES

(1) (a) Lagona, J.; Mukhopadhyay, P.; Chakrabarti, S.; Isaacs, L. The Cucurbit[*n*]uril Family. *Angew. Chem., Int. Ed.* **2005**, *44*, 4844−4870. (b) Cong, H.; Ni, X.-L.; Xiao, X.; Huang, Y.; Zhu, Q.-J.; Xue, S.-F.; Tao, Z.; Lindoy, L. F.; Wei, G. Synthesis and Separation of Cucurbit[*n*]urils and Their Derivatives. *Org. Biomol. Chem.* **2016**, *14*, 4335−4364. (c) Kim, J.; Jung, I. S.; Kim, S. Y.; Lee, E.; Kang, J. K.; Sakamoto, S.; Yamaguchi, K.; Kim, K. New Cucurbituril Homologues: Syntheses, Isolation, Characterization, and X-ray Crystal Structures of Cucurbit[*n*]uril (*n* = 5, 7, and 8). *J. Am. Chem. Soc.* **2000**, *122*, 540−541. (d) McCune, J. A.; Rosta, E.; Scherman, O. A. Modulating the Oxidation of Cucurbit[*n*]urils. *Org. Biomol. Chem.* **2017**, *15*, 998−1005.

(2) (a) Dsouza, R. N.; Pischel, U.; Nau, W. M. Fluorescent Dyes and Their Supramolecular Host/Guest Complexes with Macrocycles in Aqueous Solution. *Chem. Rev.* **2011**, *111*, 7941−7980. (b) Barrow, S. J.; Kasera, S.; Rowland, M. J.; Del Barrio, J.; Scherman, O. A. Cucurbituril-Based Molecular Recognition. *Chem. Rev.* **2015**, *115*, 12320−12406. (c) Özkan, M.; Kumar, Y.; Keser, Y.; Hadi, S. E.; Tuncel, D. Cucurbit[7]uril-Anchored Porphyrin-Based Multifunctional Molecular Platform for Photodynamic Antimicrobial and Cancer Therapy. *ACS Appl. Bio Mater.* **2019**, *2*, 4693−4697.

(3) Flinn, A.; Hough, G. C.; Stoddart, J. F.; Williams, D. J. Decamethylcucurbit[5]uril. *Angew. Chem., Int. Ed. Engl.* **1992**, *31*, 1475−1477.

(4) (a) Zhao, J.; Kim, H.-J.; Oh, J.; Kim, S.-Y.; Lee, J. W.; Sakamoto, S.; Yamaguchi, K.; Kim, K. Cucurbit[*n*]uril Derivatives Soluble in Water and Organic solvents. *Angew. Chem., Int. Ed.* **2001**, *40*, 4233−4235. (b) Wu, F.; Wu, L.-H.; Xiao, X.; Zhang, Y.-Q.; Xue, S.-F.; Tao, Z.; Day, A. I. Locating the Cyclopentano Cousins of the Cucurbit-[*n*]uril Family. *J. Org. Chem.* **2012**, *77*, 606−611.

(5) Yu, Y.; Li, J.; Zhang, M.; Cao, L.; Isaacs, L. Hydrophobic Monofunctionalized Cucurbit[7]uril Undergoes Self-inclusion Complexation and Forms Vesicle-Type Assemblies. *Chem. Commun.* **2015**, *51*, 3762−3765.

(6) Wang, X.-X.; Tian, F.-Y.; Liu, M.; Chen, K.; Zhang, Y.-Q.; Zhu, Q.-J.; Tao, Z. A Water Soluble Tetramethyl-Substituted Cucurbit[8]-uril Obtained from Larger Intermediates? *Tetrahedron* **2019**, *75*, 130488.

(7) Jon, S. Y.; Selvapalam, N.; Oh, D. H.; Kang, J. K.; Kim, S. Y.; Jeon, Y. J.; Lee, J. W.; Kim, K. Facile Synthesis of Cucurbit[*n*]uril Derivatives via Direct Functionalization: Expanding Utilization of Cucurbit[*n*]uril. *J. Am. Chem. Soc.* **2003**, *125*, 10186−10187.

(8) Shetty, D. J. K.; Park, K. M.; Kim, K. Can We Beat the Biotin−Avidin Pair?: Cucurbit[7]uril-Based Ultrahigh Affinity Host−Guest Complexes and Their Applications. *Chem. Soc. Rev.* **2015**, *44*, 8747−8761.
(9) Kaifer, A. E. Toward Reversible Control of Cucurbit[*n*]uril Complexes. *Acc. Chem. Res.* **2014**, *47*, 2160−2167.
(10) Sun, C.; Zhang, H.; Li, S.; Zhang, X.; Cheng, Q.; Ding, Y.; Wang, L.-H.; Wang, R. Polymeric Nanomedicine with "Lego" Surface Allowing Modular Functionalization and Drug Encapsulation. *ACS Appl. Mater. Interfaces* **2018**, *10*, 25090−25098.
(11) Liu, J.; Lan, Y.; Yu, Z.; Tan, C. S. Y.; Parker, R. M.; Abell, C.; Scherman, O. A. Cucurbit[*n*]uril-Based Microcapsules Self-Assembled within Microfluidic Droplets: A Versatile Approach for Supramolecular Architectures and Materials. *Acc. Chem. Res.* **2017**, *50*, 208−217.
(12) Elbashir, A. A.; Aboul-Enein, H. Y. Supramolecular Analytical Application of Cucurbit[*n*]urils Using Fluorescence Spectroscopy. *Crit. Rev. Anal. Chem.* **2015**, *45*, 52−61.
(13) Park, K. M.; Hur, M. Y.; Ghosh, S. K.; Boraste, D. M.; Kim, S.; Kim, K. Cucurbit[*n*]uril-Based Amphiphiles That Self-Assemble into Functional Nanomaterials for Therapeutics. *Chem. Commun.* **2019**, *55*, 10654−10664.
(14) Ayhan, M. M.; Karoui, H.; Hardy, M.; Rockenbauer, A.; Charles, L.; Rosas, R.; Udachin, K.; Tordo, P.; Bardelang, D.; Ouari, O. Comprehensive Synthesis of Monohydroxy−Cucurbit[*n*]urils (*n* = 5, 6, 7, 8): High Purity and High Conversions. *J. Am. Chem. Soc.* **2015**, *137*, 10238−10245.
(15) Ayhan, M. M.; Karoui, H.; Hardy, M.; Rockenbauer, A.; Charles, L.; Rosas, R.; Udachin, K.; Tordo, P.; Bardelang, D.; Ouari, O. Correction to "Comprehensive Synthesis of Monohydroxy−Cucurbit[*n*]urils (n = 5, 6, 7, 8): High Purity and High Conversions. *J. Am. Chem. Soc.* **2016**, *138*, 2060−2060.
(16) Shen, F.-F.; Chen, K.; Zhang, Y.-Q.; Zhu, Q.-J.; Tao, Z.; Cong, H. Mono-and Dihydroxylated Symmetrical Octamethylcucurbiturils and Allylated Derivatives. *Org. Lett.* **2016**, *18*, 5544−5547.
(17) Wang, X.-X.; Chen, K.; Shen, F.-F.; Wang, Y.; Zhang, Y.-Q.; Tao, Z.; Cong, H. Mono-, Di-, and Tri-Hydroxylated Symmetrical Hexamethylcucurbit[3,3]uril and Allylated Derivatives. *Eur. J. Org. Chem.* **2017**, *2017*, 6980−6985.
(18) (a) Lou, X.-Y.; Song, N.; Yang, Y.-W. Fluorescence Resonance Energy Transfer Systems in Supramolecular Macrocyclic Chemistry. *Molecules* **2017**, *22*, 1640. (b) Yesilgul, N.; Seven, O.; Guliyev, R.; Akkaya, E. U. Energy Harvesting in a Bodipy-Functionalized Rotaxane. *J. Org. Chem.* **2018**, *83*, 13228−13232. (c) Guo, S.; Song, Y.; He, Y.; Hu, X.-Y.; Wang, L. Highly Efficient Artificial Light-Harvesting Systems Constructed in Aqueous Solution Based on Supramolecular Self-Assembly. *Angew. Chem., Int. Ed.* **2018**, *57*, 3163−3167.
(19) Sun, J.; Hua, B.; Li, Q.; Zhou, J. Yang, Acid/Base-Controllable FRET and Self-Assembling Systems Fabricated by Rhodamine B Functionalized Pillar[5]arene-Based Host−Guest Recognition Motifs. *Org. Lett.* **2018**, *20*, 365−368.
(20) Li, M.; Lee, A.; Kim, K. L.; Murray, J.; Shrinidhi, A.; Sung, G.; Park, K. M.; Kim, K. Autophagy Caught in the Act: A Supramolecular FRET Pair Based on an Ultrastable Synthetic Host−Guest Complex Visualizes Autophagosome−Lysosome Fusion. *Angew. Chem., Int. Ed.* **2018**, *57*, 2120−2125.
(21) Zhao, Q.; Liu, Y. Tunable Photo-Luminescence Behaviors of Macrocycle-Containing Polymer Networks in the Solid-State. *Chem. Commun.* **2018**, *54*, 6068−6071.
(22) Li, J.-J.; Chen, Y.; Yu, J.; Cheng, N.; Liu, Y. A Supramolecular Artificial Light-harvesting System with Ultrahigh Antenna Effect. *Adv. Mater.* **2017**, *29*, 1701905.
(23) (a) Branná, P.; Černochová, J.; Rouchal, M.; Kulhánek, P.; Babinský, M.; Marek, R.; Nečas, M.; Kuřitka, I.; Vícha, R. Cooperative Binding of Cucurbit[*n*]urils and *β*-Cyclodextrin to Heteroditopic Imidazolium-Based Guests. *J. Org. Chem.* **2016**, *81*, 9595−9604. (b) Ke, C.; Smaldone, R. A.; Kikuchi, T.; Li, H.; Davis, A. P.; Stoddart, J. F. Quantitative Emergence of Hetero[4]rotaxanes by Template-Directed Click Chemistry. *Angew. Chem., Int. Ed.* **2013**, *52*, 381−387. (c) Yu, X.; Liang, W.; Huang, Q.; Wu, W.; Chruma, J. J.; Yang, C. Room-Temperature Phosphorescent *γ*-Cyclodextrin-Cucurbit[6]uril-Cowheeled [4]rotaxanes for Specific Sensing of Tryptophan. *Chem. Commun.* **2019**, *55*, 3156−3159.
(24) Li, Z.; Sun, S.; Liu, F.; Pang, Y.; Fan, J.; Song, F.; Peng, X. Large Fluorescence Enhancement of a Hemicyanine by Supramolecular Interaction with Cucurbit [6] uril and its Application as Resettable Logic Gates. *Dyes Pigm.* **2012**, *93*, 1401−1407.
(25) (a) Zhang, Y.-M.; Liu, Y.-H.; Liu, Y. Cyclodextrin-Based Multistimuli-Responsive Supramolecular Assemblies and Their Biological Functions. *Adv. Mater.* **2020**, *32*, 1806158. (b) Fu, H.-G.; Chen, Y.; Yu, Q.; Liu, Y. A Tumor-Targeting Ru/Polysaccharide/Protein Supramolecular Assembly with High Photodynamic Therapy Ability. *Chem. Commun.* **2019**, *55*, 3148−3151.
(26) Sun, J.; Shao, L.; Zhou, J.; Hua, B.; Zhang, Z.; Li, Q.; Yang, J. Efficient Enhancement of Fluorescence Emission via TPE Functionalized Cationic Pillar [5] arene-Based Host−Guest Recognition-Mediated Supramolecular Self-Assembly. *Tetrahedron Lett.* **2018**, *59*, 147−150.
(27) Sun, H.-L.; Chen, Y.; Han, X.; Liu, Y. Tunable Supramolecular Assembly and Photoswitchable Conversion of Cyclodextrin/Diphenylalanine-Based 1D and 2D Nanostructures. *Angew. Chem., Int. Ed.* **2017**, *56*, 7062−7065.

https://dx.doi.org/10.1021/acs.joc.9b03513
J. Org. Chem. 2020, 85, 6131−6136